eJNDT e-Journal of Nondestructive Testing - ISSN 1435-4934 - www.ndt.net

EWSHM 2024
11th European Workshop on Structural Health Monitoring

Reducing Artefacts in FRF-based Damage Detection Using Novel Mode Extraction Approach for Guided Ultrasonic Waves

Thomas ROLOFF [1], Jörn FROBÖSE [1], Christian HÜHNE [1], Michael SINAPIUS [1]
[1] Institute of Mechanics and Adaptronics, Technische Universität Braunschweig, Braunschweig, Germany, thomas.roloff@tu-braunschweig.de

Abstract. Damage in thin-walled structures can be detected by guided ultrasonic wave (GUW) based structural health monitoring systems. The application of phased arrays enables the scanning of large-scale structures from a single position. However, physical wave focusing requires a lot of effort. This can be significantly reduced if frequency response functions (FRFs) are used. They enable the calculation of virtual response signals for virtual focusing on any position. Although this technique offers an energy-efficient and fast possibility of damage detection, it has the disadvantage of artefacts that occur due to the multimodal nature of GUW, as damage detection is generally designed for single-mode signals. These artefacts are often reduced by mode-selective excitation/sensing or by subtracting a baseline measurement.

This work presents a concept to combine an existing FRF-based damage detection algorithm and a previously presented method for mode extraction. It enables the extraction of GUW mode components from broadband, temporally sampled, single-input single-output sensor data during signal processing on the basis of the respective dispersion relations. The aim is to reduce artefacts without using mode-selective excitation/sensing or baseline measurements. A finite element simulation of GUW propagation in an isotropic structure is used to demonstrate the advantages and limitations of this approach. The simulations include multimodal and single mode evaluation to point out the added value of performing mode extraction prior to damage detection.

It is supposed that the successful extraction of the mode components from the temporally sampled data results in a decreasing amplitude of the occurring artefacts compared to the multimodal case, while the case of mode-selective excitation apparently results in no artefacts.

The presented concept of adding mode extraction to damage detection algorithms can lead to an increase in performance of FRF-based phased array systems. Artefacts that would lead to false detection of damage are reduced inherently during signal processing which eliminates the need for mode-selective excitation/sensing or baseline measurements.

Keywords: guided ultrasonic waves, structural health monitoring, phased array, damage detection, mode extraction

https://doi.org/10.58286/29821

Introduction

Structural health monitoring (SHM) is a powerful tool to assess the integrity of technical structures. Their health state can be used to realise predictive maintenance schedules that overcome the drawbacks of current time-based maintenance approaches, by detecting and evaluating damage in time. There are numerous concepts for damage detection that vary depending on the physical principles used, the data available and the type of structure.
In the use case of thin-walled, lightweight structures, guided ultrasonic waves (GUW) are prominent as they can be used to inspect large areas of a structure because they travel long distances with low attenuation [1]. They are dispersive and occur in symmetric and antisymmetric modes with different wavenumbers at the same frequency. Additionally, GUW interact with changes in acoustical impedance such as structural edges, components and damage in form of reflections, scattering, attenuation, phase shift and mode conversion [2]. These interactions can be exploited for detection, localisation, characterisation as well as size and severeness evaluation of damage.

Wide spread sensor networks cover a large part of the structural area [3] and thus exhibit a good spatial resolution of damage detection, but assembly is complex. Another approach is to use phased arrays, a setup consisting of multiple transducers that are arranged in a locally dense manner and are used to physically or virtually steer the GUW propagation for a directive damage detection [4].

Most GUW-based SHM approaches, as well as most phased array methods, assume a predominantly single mode GUW propagation to reduce the influence of multimodal responses that reduces the damage detection accuracy. Nevertheless, if the assumption of single mode GUW propagation is not applicable and multiple mode wave packages appear in the time domain signal, they are not easily separable. If both mode components remain in the signal, the wave packages corresponding to the mode other than the evaluated mode will be analysed with an incorrectly assumed propagation velocity. This in turn leads to an incorrect approximation of the distance and location, which manifests itself in the form of artefacts in damage detection.

The aim of this work is to present a concept to combine a frequency response function (FRF) based phased array damage detection algorithm with a mode extraction method that uses temporally sampled single-input single-output data and the respective dispersion relations. The advantages of this combination are presented and evaluated for further investigations.

1. FRF-based Damage Detection Algorithm

The FRF-based damage detection algorithm used in this work relies on the work of Kudela et al. [5]. The amplitude-based approach uses pulse echo signals in a two-dimensional array setup and designs excitation signals in such a way that the energy is focused on an inspection point. It is assumed that a wave package is reflected if the inspection point is part of a reflective interface, i.e. structural edge, defect, etc. By focusing on multiple points, damage indices for every position can be calculated to form a damage index heat map indicating possible reflector positions.

The method mainly relies on the dispersion compensation of the corresponding signals for a high spatial resolution, while the compensation is only performed for a single mode. The three main steps of the method are as follows. First, in a pre-compensation stage, excitation signals are designed for every array element so that the desired wave form of a short pulse arrives at the focus position after dispersive propagation from the transmitter to the inspection point. Second, in a post-compensation stage, the response signals are

measured. Again, the distance between the inspection point and the receiver is used to compensate the dispersion and calculate a non-dispersive response of the signal possibly reflected at the inspection position. Third, the damage index for every focusing position is calculated by summing up the absolute value of the Hilbert envelope of all dispersion compensated signals. If the inspection point is a reflector it will have a non-zero amplitude, if there is no reflector, the amplitude will be close to zero.

While Kudela et al. used physical focusing for every inspection point, Yang et al. [6] introduced the use of FRFs. Under the assumption of linear systems and GUW propagation, they enable the calculation of virtual response signals which significantly reduces the experimental effort to inspect large areas with a high spatial resolution.

Another extension is proposed by Lang et al. [7] in form of the focusing phase imaging method by using the instantaneous phase information. The authors assume that in the case of the coincidence of inspection point and defect, the instantaneous phases of the individual response signals coincide. For a detailed description of the method it is referred to [7]. In the publication, improved damage detection was demonstrated compared to the amplitude-based method for experimentally determined data with an aluminium plate and two round holes. In particular, the phase imaging method is able to better suppress side lobes and also shows no blind areas or artefacts due to plate edge reflections.

However, both publications assume predominantly single mode GUW propagation by tuning the frequency so that the transmitters mainly emit one of the two wave modes. While the focusing phase imaging seems to suppress artefacts, the amplitude-based damage detection suffers from erroneous damage localisation if wave packages from the mode that is not evaluated occur in the signal. An erroneous propagation velocity is assumed which results in a false distance approximation and damage localisation. These artefacts are removed by subtracting baseline measurements. These might not always be available. Here, the novel mode extraction algorithm comes into play. The following paragraph gives a brief overview of the method developed to extract single mode GUW signals.

2. Mode Extraction Algorithm

In most cases, mode selectivity is achieved by frequency tuning, two-sided transducer setups or complex hardware such as interdigital transducers as well as spatially distributed measurements using laser vibrometry or air-coupled ultrasound techniques.

The framework presented here is an extension of two methods for extracting signal components based on group delay (GD) estimations. On the one hand, the frequency-domain intrinsic component decomposition (FICD) algorithm [8] is used. It offers a possibility to identify nonlinear and non-monotonic GDs in the frequency domain with generic kernel functions and also offers the possibility to separate and reconstruct the associated signal components with time-frequency filters. On the other hand, the iterative frequency domain envelope-tracking filter (IFETF) algorithm [9] is considered. This is also suitable for separating and reconstructing individual signal components, but uses a different generic method for identifying the GDs and also enables an iterative improvement of the time-frequency resolution of the GD estimations. In this paper, the mentioned algorithms are extended to the dispersion-based frequency-domain intrinsic component decomposition (DBFICD) algorithm [10] by taking into account the dispersion relations. The aim of the extension is to approximate the GD ridges on a physical basis using the dispersion relations. The general procedure is as follows. In the first step, pseudo impulse response functions (IRF, pseudo indicates a limited frequency bandwidth) are determined energy-efficiently using a sweep excitation and transforming the respective FRF into an IRF by inverse Fourier transform. Afterwards, a mode-selective dispersion-based ridge extraction (MDBRE) is

performed in the time frequency representation. The frequency envelope is estimated using a Fourier series basis for mode reconstruction. The results are refined using the IFETF algorithm and the reconstructed S_0 mode and A_0 mode components are combined to form mode-selective IRFs. These enable the calculation of mode-selective virtual responses. For a detailed description of the method it is referred to [10].

Fig. 1 shows an exemplary result of the DBFICD mode extraction. To get information on the experimental setup used it is referred to [10]. The short-time Fourier transform (STFT) of the multimodal pseudo IRF for a transmitter-receiver pair with a distance of 700 mm applied on a 3 mm aluminium plate is shown on the left of Fig. 1. The pseudo IRF is determined using a sweep signal with a bandwidth from 50 – 350 kHz. The STFT of the extracted, mode-selective A_0 mode pseudo IRF $h_{A_0}(t)$ is shown on the right of Fig. 1. This can be used to calculate virtual single mode response signals $u_{A_0}(t)$ from an excitation signal $f(t)$ in the corresponding frequency range

$$u_{A_0}(t) = h_{A_0}(t) * f(t).$$

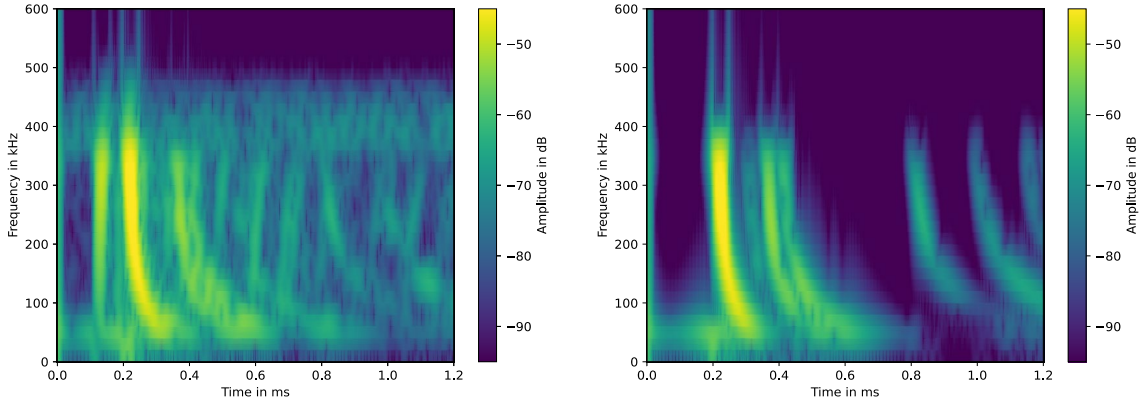

Fig. 1: STFT results of DBFICD mode extraction algorithm on 50 – 350 kHz pseudo IRF in an isotropic aluminium plate, for setup see [10]. Left) Multimodal response. Right) Extracted A_0 mode response.

3. Numerical Model

The aim is to have a numerical model that enables parameter studies to investigate different influences on the performance of the damage detection.

ABAQUS Explicit is used to model the GUW propagation in a 1,000 x 1,000 x 3 mm³ isotropic plate made out of aluminium alloy 1100 (density 2,710 kg/m³, Young's modulus 69 GPa, Poisson's ratio 0.33). A representation of the numerical model is depicted in Fig. 2. For defect simulation, a 15 mm diameter through hole is positioned with its centre at (635.4 mm, 673.4 mm). C3D8R elements are used and the meshing is adapted to the smallest occurring wavelength (7.49 mm, A_0 mode at 300 kHz) in the investigated frequency range up to 300 kHz. 16 elements per wavelength are used in the x-y-plane and 8 elements are used in thickness direction, leading to an element size of 0.468 x 0.468 x 0.375 mm³. The meshing is a result of a convergence study in a 2D simulation by comparing simulated to analytically determined dispersion diagrams. The difference between the determined wavenumbers is below 1 %.

A circular transducer array of 9 elements is realised in the middle of the plate with a radius of 55 mm. The transducers are simplified as point forces and point-wise sensors by reading out the three displacement components with the orientation being depicted in Fig. 2. While the excitation takes place at the top of the plate, the displacements are tracked at both surfaces at the respective sensor positions to calculate mode-selective responses. In this

setup, only one simulation is necessary to obtain multimodal, symmetric and antisymmetric response signals. For the symmetric responses, the top (u_{top}) and bottom (u_{bot}) displacement signals are subtracted for the out-of-plane component and added for the in-plane components and vice versa for the antisymmetric responses. This exploits the phase relations of in- and out-of-phase oscillations of propagating symmetric and antisymmetric GUW signals.

Impulse signals are used for excitation in the simulation. To get all IRFs in the phased array, nine simulations are necessary. In a round robin fashion, the transducers are used as excitation while all positions are read out as sensors in every simulation.

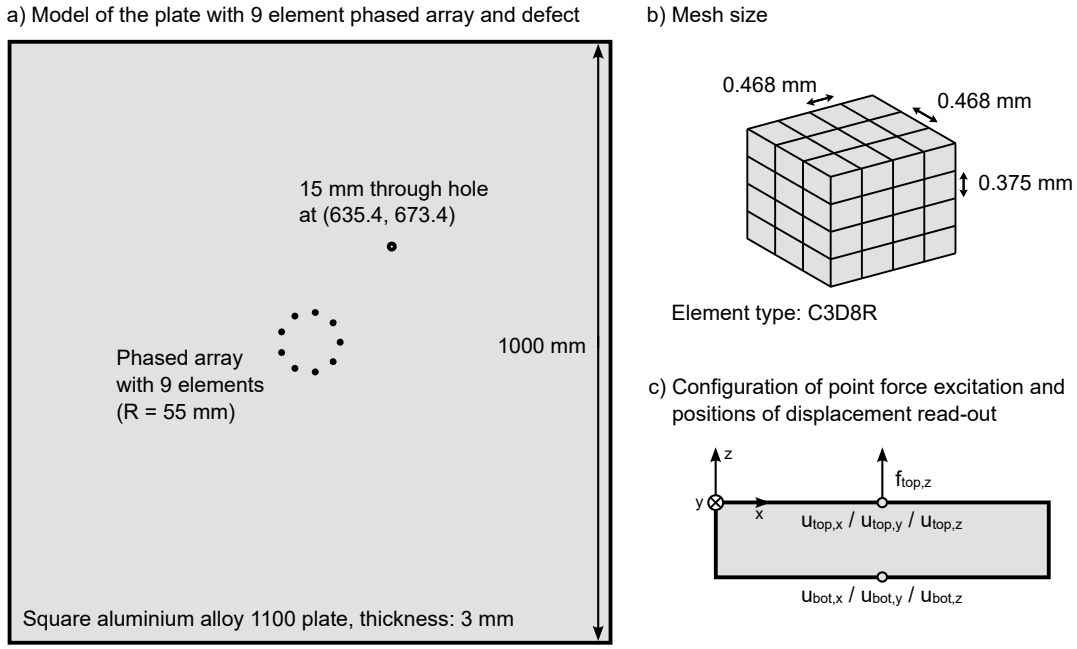

Fig. 2: Numerical model used to simulate GUW propagation and phased array responses with ABAQUS Explicit, mesh size and excitation / read-out configuration to get symmetric and antisymmetric signals

To investigate the influence of different modes on the damage detection, three GUW detection cases are investigated (both modes, exclusively antisymmetric or symmetric mode) and in all cases the dispersion compensation is performed according to [5], [6] for the A_0 mode as it has smaller wavelengths and is thus more sensitive for smaller damage. The aim is to show the influence of mode selectivity on artefacts and display possible advantages of using mode extraction prior to damage detection.

4. Results

In this section, the damage detection results are presented for the numerically determined signals and the amplitude-based phased array approach [5,6]. The simulation results in IRFs for all 81 combinations of transducers in the nine element array for all three dimensions. In this case, the in-plane GUW propagation is evaluated by calculating damage indices in x- and y-direction and combining them. The IRFs are used to virtually calculate the focused responses to a 2-cycle Hanning-windowed sine burst with a centre frequency of 120 kHz.

Fig. 3 presents the damage index maps for the three evaluation cases of multimodal, antisymmetric and symmetric GUW responses while the dispersion compensation of the signals is performed for the A_0 mode. The x- and y-axis present the square plates edges and the colour code illustrates the normalised damage index. The white circle at (635.4 mm, 673.4 mm) has a diameter of 15 mm and depicts the through hole investigated in this study.

On the left and in the middle of Fig. 3, the results for a multimodal and A_0 mode GUW propagation are shown, respectively, that depict high damage values in the vicinity of the transducer array and a circular ring with the diameter of the plates edge dimensions. Both damage index maps show a brighter area around the damage and a circular shadow with a radius approximately the distance between the middle of the array and damage.

The result for S_0 mode propagation, but A_0 mode evaluation is presented in Fig. 3. Here, the bright area inside the array vanishes and two circular bright areas appear with the inner ring showing a higher damage index and a radius of approximately 250 mm while the outer ring has a radius of approximately 500 mm.

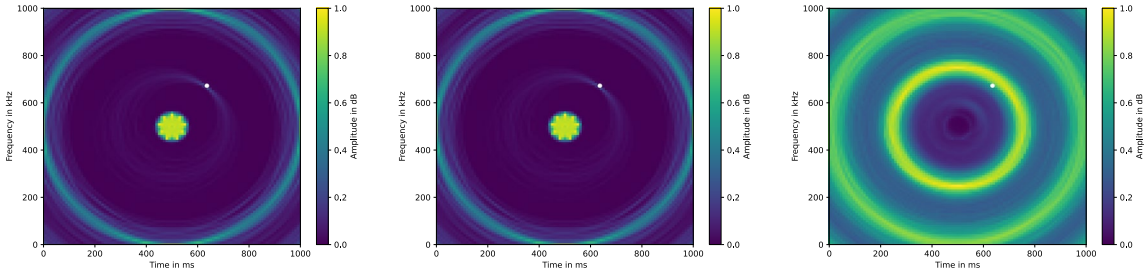

Fig. 3: Damage index maps for FRF-based phased array approach on in-plane data with 2-cycle Hanning windowed sine burst at 120 kHz. Left) Multimodal propagation, A_0 mode evaluation. Middle) A_0 propagation, A_0 mode evaluation. Right) S_0 propagation, A_0 mode evaluation.

The array interaction with itself and the edge reflections outshine the area of interest. Therefore, a passepartout with inner radius of 70 mm and outer radius of 390 mm is applied to exclude artefacts from direct paths between transducers and edge reflections and increase visibility in the area of interest. The results are shown in Fig. 4. After updated normalisation of the damage index, the damage detection becomes more visible.

The clearest results occur for the case with A_0 mode propagation and evaluation, which can be seen in the middle of Fig. 4. The brightest area coincides with the damage and the maximum occurs at the interaction plane of the hole pointing to the array. However, the result is not perfectly concentrated but presents a shadow around the array with the radius being approximately the distance between array and defect. The same is valid for the evaluation of the A_0 mode under multimodal propagation as shown on the left of Fig. 4, but in this case, there is more background noise and a slightly visible shadow occurs right behind the defect. The same shadow occurs in the results for S_0 mode propagation and A_0 mode evaluation as presented on the right of Fig. 4. However, it appears in a full circle and has a close to uniform amplitude.

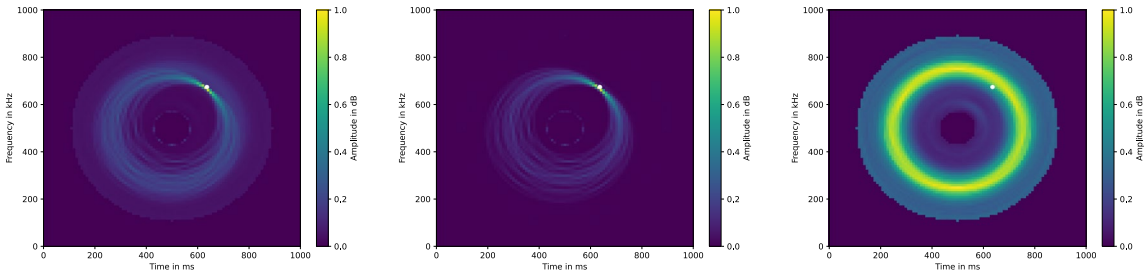

Fig. 4: Damage index maps (incl. passepartout) for FRF-based phased array approach on in-plane data with 2-cycle Hanning windowed sine burst at 120 kHz. Left) Multimodal propagation, A_0 mode evaluation. Middle) A_0 propagation, A_0 mode evaluation. Right) S_0 propagation, A_0 mode evaluation.

5. Discussion

The results confirm the findings of Yang et al. [6] even though they use PZT sensors that are sensitive for in- and out-of-plane motion, but mainly in-plane components. The influence of different motion orientations is discussed in the following. The interactions and reflections of the array elements results in a blind spot in the vicinity of the array and the edge reflections outshine the damage case. The circular shape of the edge reflections in Fig. 3 can be explained by the grating lobes of the array as the distance between two adjacent array elements of 37.62 mm is significantly bigger than the wavelength of the A_0 mode at 120 kHz with 13.78 mm. Therefore, the strong edge reflections at x=500 mm and y=500 mm also appear in other directions.

It is evident that the most precise damage detection results can be achieved when the A_0 mode is evaluated under single mode A_0 propagation. The shadow that occurs can again be explained by the grating lobes. Additionally, unexpected phase shifts in the motion of the nodes in the vicinity of the point force excitation for the numerical model result in slightly erroneous dispersion compensation that basically relies on phase shifting.

For multimode GUW propagation and A_0 mode evaluation the results become slightly blurrier. This can be explained as more components belonging to the S_0 mode occur and blur the result. However, the A_0 mode components exhibit a higher amplitude which is why the blurring is not so prominent. The A_0 mode has a significantly higher out-of-plane particle motion in this frequency range than the S_0 mode and as the excitation is realised as an out-of-plane point-force, the A_0 mode is excited more efficiently. The S_0 mode has higher in-plane components. The in-plane evaluation is selected as the aim is to investigate occurring artefacts that appear more prominently if the amplitude of A_0 and S_0 mode are similar. The shadow occurring right behind the damage belongs to an erroneous evaluation of S_0 mode components, as the same shadow can be found on the right of Fig. 3 and Fig. 4.

Under S_0 mode propagation and A_0 mode evaluation, no damage detection is possible at all. The two circular areas of high damage index outshine the other areas. Both rings on the right of Fig. 3 correspond to first and second order edge reflections of the S_0 mode which explains why the inner ring is brighter. The circular shape results from the grating lobes of the array. The radii of the rings with the inner one being half as big as the outer one can be explained by the difference in energy velocity at 120 kHz as the one of the S_0 mode (5315.54 m/s) is approximately two times higher than the one of the A_0 mode (2699.67 m/s). Therefore, the distances of the first and second edge reflection are underestimated by a factor of two.

It needs to be noted that the current numerical setup produces strong grating lobes at the selected frequency due to the ratio of distance between the transducers and the occurring wavelength. To overcome this drawback, different frequencies, modes and distances between phased array elements have to be investigated. Additionally, artefacts that are the main focus of this work are most prominent when the amplitude of S_0 and A_0 mode components are similar. Therefore, further simulations will be designed in such a way that the S_0 and A_0 mode have similar in- or out-of-plane components.

Conclusion

In this work, influences of multimodal GUW propagation and incorrectly assumed mode components on damage detection using phased arrays are presented. An approach is proposed to combine the damage detection with a mode extraction algorithm that relies on single-input single-output data and enables the extraction of single mode IRFs. These can be used to calculate single mode virtual signals, remove artefacts from damage detection methods and improve their performance. The impact of single mode responses depends on the specimen

used and the selected frequency range as it is supposedly most effective when S_0 and A_0 mode components are approximately of the same amplitude. This is subject to further research to select a simulation setup and frequency range where artefacts are even more prominent. The next step is to apply the mode extraction to the simulated data and compare mode extracted and mode-selective results. The long-term goal is to extend this concept to anisotropic wave propagation.

Funding

The authors expressly acknowledge the financial support of the research work on this article within the Research Unit 3022 “Ultrasonic Monitoring of Fiber Metal Laminates Using Integrated Sensors” by the German Research Foundation (Deutsche Forschungsgemeinschaft (DFG)), Project-ID 418311604.

References

[1] Giurgiutiu V. Structural health monitoring with piezoelectric wafer active sensors. Amsterdam: Academic Press/Elsevier; 2008.
[2] Lammering R, Gabbert U, Sinapius M, Schuster T, Wierach P (eds.). Lamb-Wave Based Structural Health Monitoring in Polymer Composites. Cham: Springer; 2018.
[3] Wang Y, Qiu L, Luo Y, Ding R, Jiang F. A piezoelectric sensor network with shared signal transmission wires for structural health monitoring of aircraft smart skin. Mechanical Systems and Signal Processing 2020;141:106730. https://doi.org/10.1016/j.ymssp.2020.106730.
[4] Yu L, Giurgiutiu V. In situ 2-D piezoelectric wafer active sensors arrays for guided wave damage detection. Ultrasonics 2008;48(2):117–34. https://doi.org/10.1016/j.ultras.2007.10.008.
[5] Kudela P, Radzienski M, Ostachowicz W, Yang Z. Structural Health Monitoring system based on a concept of Lamb wave focusing by the piezoelectric array. Mechanical Systems and Signal Processing 2018;108:21–32. https://doi.org/10.1016/j.ymssp.2018.02.008.
[6] Yang Z-B, Zhu M-F, Lang Y-F, Chen X-F. FRF-based lamb wave phased array. Mechanical Systems and Signal Processing 2022;166. https://doi.org/10.1016/j.ymssp.2021.108462.
[7] Lang Y-F, Tian S-H, Yang Z-B, Zhang W, Kong D-T, Xu K-L et al. Focusing phase imaging for Lamb wave phased array. Smart Mater. Struct. 2022;31(2). https://doi.org/10.1088/1361-665X/ac40e0.
[8] Liu Z, He Q, Chen S, Dong X, Peng Z, Zhang W. Frequency-domain intrinsic component decomposition for multimodal signals with nonlinear group delays. Signal Processing 2019;154:57–63. https://doi.org/10.1016/j.sigpro.2018.07.026.
[9] Jiang Y, Niu G. An iterative frequency-domain envelope-tracking filter for dispersive signal decomposition in structural health monitoring. Mechanical Systems and Signal Processing 2022;179:1–26. https://doi.org/10.1016/j.ymssp.2022.109329.
[10] Roloff T, Sinapius M. Generation of Mode-Selective Frequency Response Functions from Temporally Sampled, Broadband and Multimodal Guided Ultrasonic Wave Signals. In: Proceedings of the 14th International Workshop on Structural Health Monitoring. Destech Publications, Inc; 2023.